ISSN 2229-5518

Temperature and Deposition Time Dependence of the Geometrical Properties of Tin Oxide Nanostructures

Gil Nonato C. Santos, Arnel A. Salvador, Reuben V. Quiroga

Abstract—Tin Oxide nanomaterial was synthesized using the horizontal vapor phase growth (HVPG) technique. The study investigated the optimum growth parameters by varying the growth temperature from 900°C to 1200°C and growth time of 1 hour to 5 hours. The SnO_2 bulk powder with purity rate of 99.99% were placed in a sealed quartz tube with a vacuum pressure of $\approx 10^{-5}$ Torr and baked with the desired growth parameters. The resulting nanocrystals displayed different structures ranging from nanobelts to nanorods as confirmed by the SEM. Results from EDX and DTA showed that indeed the grown samples were congruent based on the atomic composition and thermal property of the nanomaterials. The XRD also verified that the crystal structure was rutile but with low indexed peaks. Using the same growth technique, samples were grown on Silicon (100) substrate and exhibited nanorods and nanobelts. The SnO_2 nanomaterial also displayed fluorescence and photoluminescence signals. The photoluminescence spectrum has a broad emission in the visible region with peaks at 558 nm and 666 nm. The visible light emission was known to be related to defect levels within the band gap of SnO_2, associated with O vacancies or Sn interstitials that have formed during the synthesis process.

Keyword —nanomaterial, horizontal vapor phase growth (HVPG) technique, photoluminescence

1 Introduction

Nanostructured semiconducting oxide materials had received broad attention due to their distinguished performance in electronics, optics and photonics. Synthesis of semiconducting oxide thin films have been an active field because of their applications as sensors, transducers, and catalysts. The studies of semiconducting oxides have been focused on two-dimensional films and zero-dimensional nanoparticles, which can be readily synthesized with various well-established techniques such as chemical vapor deposition, sol-gel processing, pulsed laser deposition, and solid state reaction.[1] In this study, the material of our particular interest is tin oxide, an n-type wide band-gap semiconductor and a key functional material that has been extensively used for optoelectronic devices and gas sensors. [1]-[2] For the gas-sensing applications, it has been shown that the synthesis of SnO_2 films under a nanostructured form considerably enhances their gas-sensing performance.

As stimulated by the novel properties of carbon nanotubes, wire-like nanostructures have attracted extensive interest over the past decade because of their great potential for addressing some basic issues about dimensionality and space-confined transport phenomena as well as applications.[5] Besides nanotubules [6]-[7], many other wire-like nanomaterials, such as carbides [SiC [8]-[10] and TiC [8], nitrides (GaN [11]-[12] and Si_3N_4[13]), compound semiconductors [14]-[15], element semiconductors (Si [16]-[18]) and Ge [16], and oxide Ga_2O_3 [23] and MgO [24] nanowires, have been successfully fabricated. In geometrical structures, these nanostructures can be classified into two main groups: hollow nanotubes and solid nanowires, which have a common characteristic of cylindrical symmetric cross section.

In this work, SnO_2 nanomaterials were grown using horizontal vapor phase growth technique. The motivations to adopt this technique over the other processes are the following: 1.) High purity materials can be grown; 2.) Source material is powder in form; 3.) Greater quantity products with less source material; 4.) No gas molecules in between; 5.) Its versatility in composition of deposit; 6.) The ability to produce unusual nanostructures; 7.) The substrate is easily installed; 8.) Has an excellent bonding to the substrate; and 9.) Elimination of pollutants and effluents which is an important ecological factor [23].

2 Experimental Section

A small amount of 0.035 grams of high purity Merck SnO_2 (99.9%) powder was weighed and loaded in a close-end quartz tube with inner size diameter of 8.5 mm, outer size diameter of 11 mm, and length of 220 mm. The quartz tube was attached to the THERMIONICS High Vacuum System and was sealed at a vacuum pressure of

- *Gil Nonato C. Santos, Doctor of Philosophy in Materials Science, Associate Professor, De La Salle University-Manila, Philippines. E-mail: santosg@dlsu.edu.ph*
- *Arnel A. Salvador, Doctor of Philosophy in Physics, Professor, University of the Philippines-Diliman. E-mail: arnelsalvador@nip.upd.edu.ph*
- *Reuben V. Quiroga, Doctor of Philosophy in Physics, De La Salle University-Manila. Email: quirogar@dlsu.edu.ph*

≈ 10^{-5} Torr. The sealed quartz tube was divided into three zones where zone 1 was set as the hottest zone based on the assigned growth temperature, while zone 2 and 3 are in deceasing temperature. The samples were grown from 900° to 1200ºC with varying growth time of 1 hour to 5 hours. The temperature profile along the tube furnace was also monitored using a Type K Thermocouple Fluke Digital Thermometer. To examine the synthesized products, the quartz tube was gently cracked and observed to be deposited at zones 2 and 3 where the fluffy white products are seen on the walls of the quartz tube using an SEM. Several samples were also collected for XRD, DTA, and Spectral Imaging measurements.

3 Results And Discussion

Figure 1 presents some of the SEM images of the silver Growth of SnO_2 nanostructure follows the SVLS (Solid-Vapor-Liquid-Solid) phase growth. The nanowire growth begins after the source material becomes supersaturated in liquid and continues as long as it remains in a liquid state. During growth, the temperature gradient directs the nanowire's growth direction and size. Ultimately, the growth terminates when the temperature is below the eutectic temperature of the source material. Figure 1 shows the SEM image of synthesized SnO_2 nanomaterial.

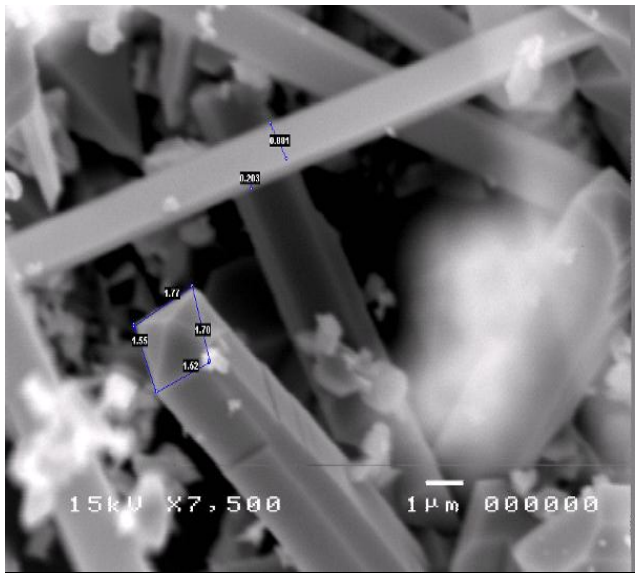

Fig. 1 SEM Image of the SnO_2 Nanomaterial grown at 1200°C for 1 hour

Also grown at 1200°C for 1 hour was the SnO_2 nanobelt. Observe in Figure 2 the prominent structure of the SnO_2 nanobelt with a measured width of 1.84 μm and thickness of 90 nm. Nanobelts are nanowires that have well-defined geometrical shape and side surfaces.

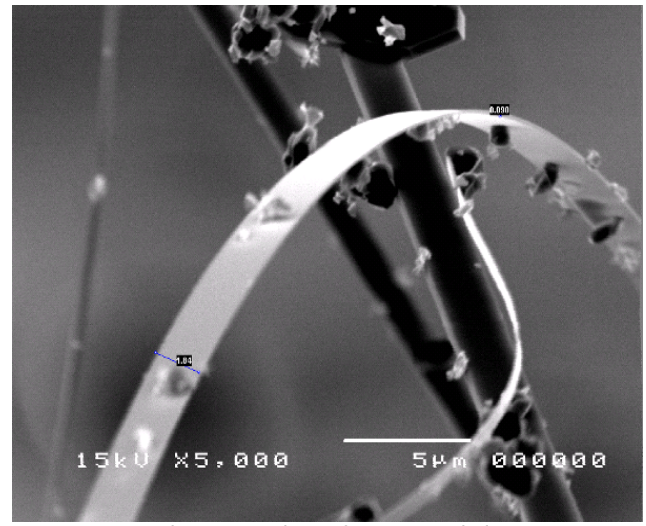

Fig. 2 SEM Photo of SnO_2 Nanobelt

Using a high resolution scanning electron microscope in Figure 3, the surface of the SnO_2 nanomaterial was observed to be porose and composed of many uniform crystalline grains of approximately25 nm in size. This surface was observed to be suitable for fabricating gas sensors because of its porosity over large surface[32].

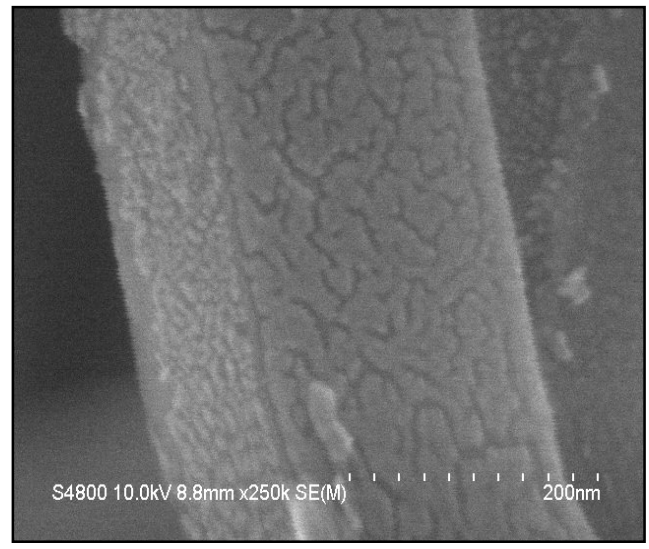

Fig. 3 High Resolution Image of the SnO_2 Nanomaterial magnified at 250,000x

The study also found that Silicon (100) can be an effective substrate for growing SnO_2 nanomaterials as shown in Figures 4 and 5. In this process, the growth direction of the nanorods was led by an epitaxial orientation defined by the substrate that determines the aligned growth. The nanorods tend to take the least mismatch orientation on the substrate to reduce the interface mismatch energy.

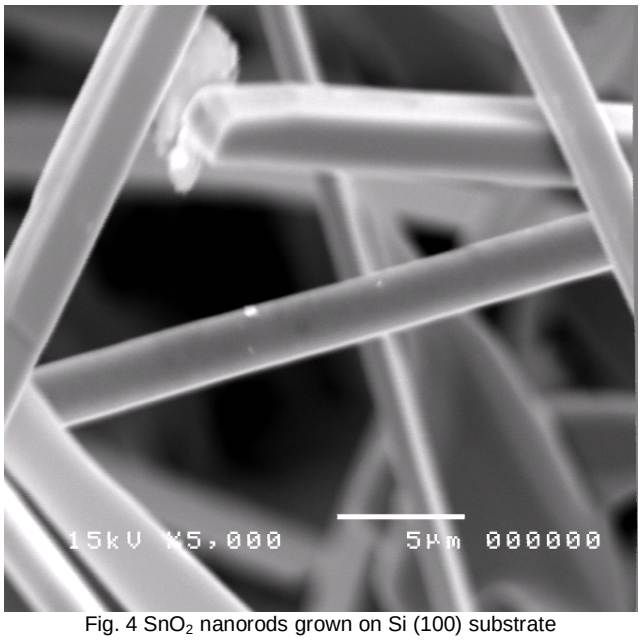

Fig. 4 SnO_2 nanorods grown on Si (100) substrate

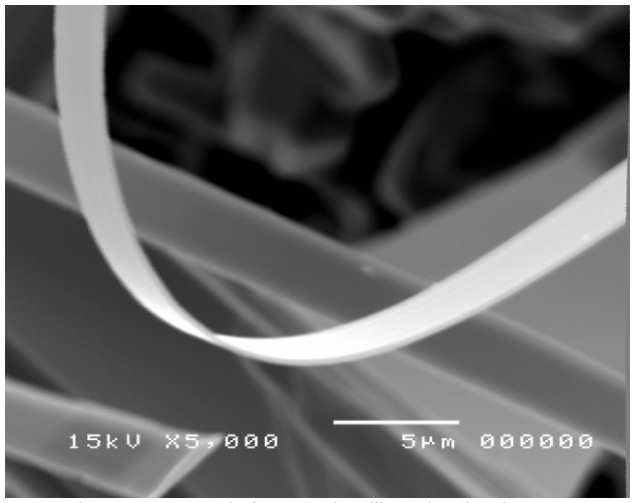

Fig. 5 SnO_2 nanobelt grown in Silicon (100) substrate

Figure 6 illustrates the EDX analysis of the SnO_2 Nanomaterial grown at Zone 3 with a growth temperature of 1200°C for 1 hour. The atomic composition of the SnO_2 nanomaterial was shown to be 1:2 indicating that the growth process was congruent with the starting materials.

Figure 7 exhibits the XRD pattern verified from the SnO_2 powder source material and the nanomaterial grown. The Miller indices are indicated on each diffraction peak. The diffraction peaks of the (110), (101), (200), (211), (220), (002), (310), (112), (301), (202), and (321) planes can be readily indexed to the tetragonal rutile structure of SnO_2 with lattice constants of a = 4.738 Å and c = 3.187 Å (JCPDS File No. 41-1445) while several XRD measurements were done to determine the crystal structure of the SnO_2 nanomaterial. The results show that it has low indexed peaks which were observed at (110), (101), and (211).

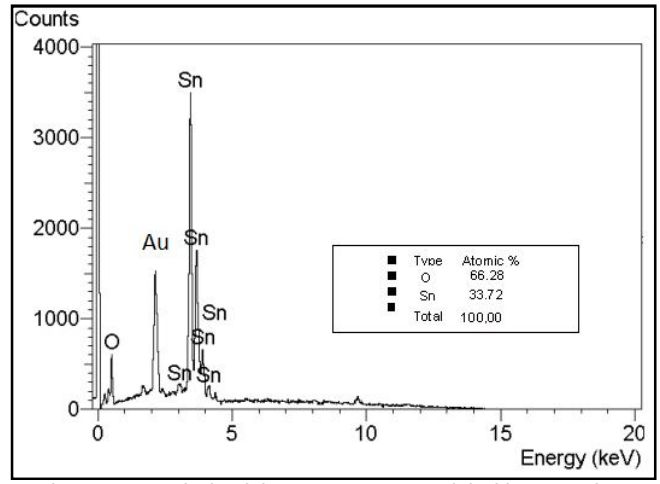

Fig. 6 EDX Analysis of the SnO_2 Nanomaterial with Au coating

All of the products including those several nanometers in size are found to be straight and bent as seen using the SEM. The SnO_2 nanomaterial has a normal rutile crystal structure wherein the SnO_2 nanorods displayed a rectangular cross section enclosed by (010) and (101) facet planes. The growth direction of these SnO_2 nanorods are parallel to the [101] crystal direction.

Figure 8 presents the DTA analysis of the SnO_2 powder and nanomaterial. From the resulting graph, it was shown that both materials had undergone a similar phase although there was a slight difference in its melting point. Thermodynamics analysis indicates that the reaction occurs at high temperature where s represents the solid state and grepresents the gas state respectively.

$$SnO_2(s) \rightarrow SnO(g) + \tfrac{1}{2}\, O_2\,(g)$$

Although SnO(*g*) was relatively stable, the following two reactions can happen spontaneously during the process

$$SnO(g) + \tfrac{1}{2}\, O_2(g) \rightarrow SnO_2(s) \quad (1)$$
$$SnO(g) \rightarrow \tfrac{1}{2}\, SnO_2(s) + \tfrac{1}{2}\, Sn(l) \quad (2)$$

Reaction 1 is a process of reoxidization of the SnO vapors while reaction 2 is a decomposition process of gas-state SnO. It is possible for both reactions to be responsible for SnO_2 products. Another oxidized reaction might also occur in the system.

$$Sn(l) + O_2 \rightarrow SnO_2(s) \quad (3)$$

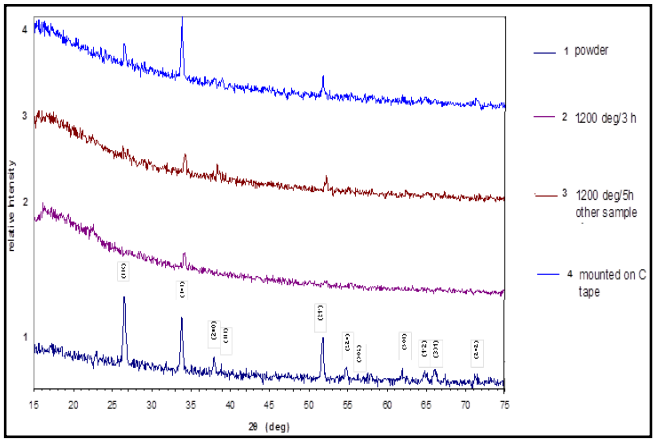

Fig. 7 XRD of the SnO_2 powder (1) and SnO_2 Nanomaterial (2-4)

Considering the oxidizing reactions (1) and (3), it is evident that oxygen preferably reacts with liquid-state Sn than the SnO vapors. In the present study, the metal Sn has been clearly identified existing in the SnO source powders after evaporation. This is an indication that the concentration of oxygen is limited in the present equipment system. The metal Sn particles are also found coexisting with SnO_2 nanobelts at the high-temperature region indicating the occurrence of the decomposition of SnO vapors. Thus, the decomposition of SnO vapors is likely the dominant process to be responsible for the formation of SnO_2 products in our system.

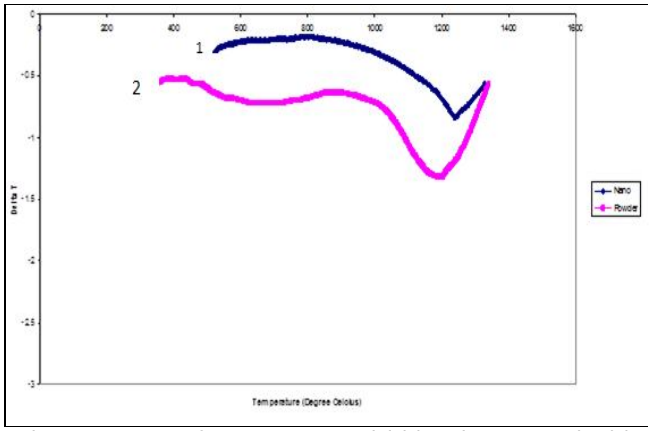

Fig. 8 DTA Curve of SnO_2 Nanomaterial (1) and SnO_2 Powder (2)

Figure 9 shows the PL spectra of the SnO_2 nanomaterial measured with a fluorescence spectrophotometer using a Xe lamp with an excitation wavelength of 325 nm at room temperature.

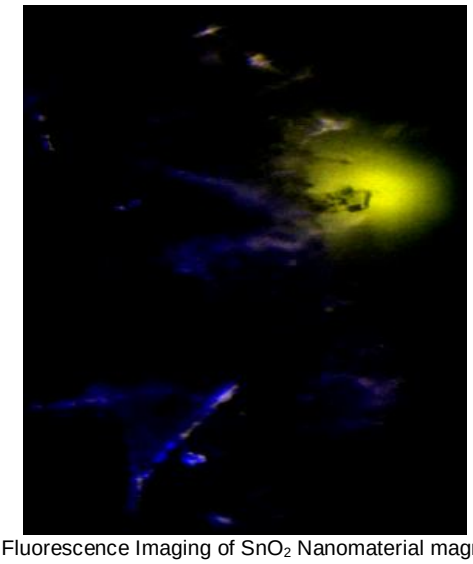

Fig. 9 Fluorescence Imaging of SnO_2 Nanomaterial magnified at 20x

The PL spectrum of the nanomaterial exhibits a strong emission peak at 666.41 nm as shown in Figure 10. Visible emissions with a peak wavelength positioned at around 558.39 nm are dominantly observed. This was known to be related to the defect levels within the band gap of SnO_2, associated with O vacancies or Sn interstitials that have formed during the synthesis process [28]. A similar emission has been reported in the case of SnO_2 nanoribbons synthesized by laser ablation30 and SnO_2 nanorods synthesized by solution phase growth [31].

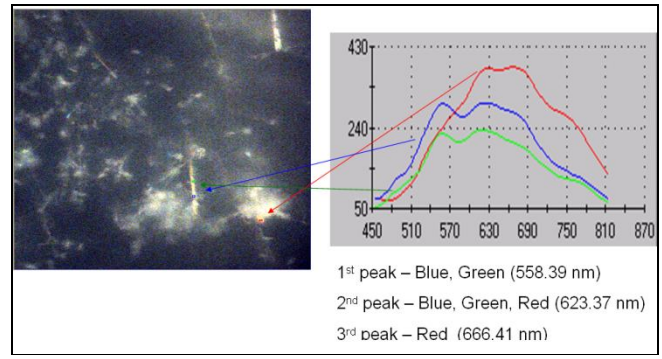

Fig. 10 Photoluminescence Imaging of SnO_2 Nanomaterial magnified at 20x

4 Conclusion

The study showed that the growth of the SnO_2 nanomaterials was successful using the HVPG technique. The nanomaterials grown were dependent on the vacuum pressure, the quartz tube used, growth temperature and time. Depending on the functionality and application of the nanomaterial, it can be concluded that the best temperature to grow SnO_2 nanomaterials was ob-

served at 1200°C. It was also relevant to consider that as the growth time increases, the amount of nanomaterials produced increases. The source material used in that synthesis was SnO_2 powder and the composition of the SnO_2 nanomaterial was similar to the starting oxide. The growth was governed by a SVLS process, in which the SnO_2 vapor which evaporated from the starting oxide at a higher temperature zone and directly grows on the quartz tube or on a substrate at a lower temperature region that produce different nanostructures. The belt-like morphology was distinct from those of semiconductor nanowires. The XRD proved that the SnO_2 nanomaterial was rutile in structure with relatively low indexed peaks. With a well-defined geometry and perfect crystallinity, the SnO_2 nanobelts are likely to be a model material for a systematic experimental and theoretical understanding in the fundamental electrical, thermal, optical, and ionic transport processes in wirelike nanostructures with the absence of dislocations and defects.

REFERENCES

[1] F. S. Galasso, Structure and Properties of Inorganic Solids (Pergamon, New York, 1970).
[2] A provisional patent has been led by Georgia Tech Research Cooperation.
[3] D. S. Ginley, C. Bright, Mater. Res. Soc. Bull. 25, 15 (2000).
[4] N. Yamazoe, Sens. Actuators B 5, 7 (1991).
[5] C. Dekker, Phys. Today 52, 22 (1999).
[6] S. Iijima, Nature 354, 56 (1991).
[7] Y. Feldman, E. Wasserman, D. J. Srolovitz, R. Tenne, Science 267, 222 (1995).
[8] H. J. Dai et al., Nature 375, 769 (1995).
[9] Z. W. Pan et al., Adv. Mater. 12, 1186 (2000).
[10] Z. L. Wang et al., Appl. Phys. Lett. 77, 3349 (2000).
[11] W. Han, S. Fan, Q. Li, Y. Hu, Science 277, 1287 (1997).
[12] X. F. Duan, C. M. Lieber, J. Am. Chem. Soc. 122, 188 (2000).
[13] W. Q. Han et al., Appl. Phys. Lett. 71, 2271 (1997).
[14] X. F. Duan, C. M. Lieber, Adv. Mater. 12, 298 (2000).
[15] X. F. Duan, Y. Huang, Y. Cui, J. Wang, C. M. Lieber, Nature 409, 66 (2001).
[16] A. M. Morales, C. M. Lieber, Science 279, 208 (1998).
[17] S. T. Lee, N. Wang, Y. F. Zhang, Y. H. Tang, Mater. Res. Soc. Bull. 24, 36 (1999).
[18] D. P. Yu et al., Solid State Commun. 105, 403 (1998).
[19] H. Z. Zhang et al., Solid State Commun. 109, 677 (1999).
[20] P. Yang, C. M. Lieber, J. Mater. Res. 12, 2981 (1997).
[21] The Sn nanoparticles are adhered on the surfaces of the belts rather than at the ends, in contrast to the nanowires prepared by VLS reaction (12-14) that always terminate at one end with a catalytic nanoparticle. The formation of the Sn nanoparticles is believed to be related to the decomposition of the SnO_2 or SnO vapor.
[22] P. B. Hirsch, A. Howie, R. B. Nicholson, D. W. Pashley, M. L. Whelan, Electron Microscopy of Thin Crystals (Krieger, New York, 1977).
[23] The Ga_2O_3 nanobelts can be prepared by either heating mixed Ga_2O_3 powder at 1000ºC or heating GaN powders at 950ºC. The products prepared from the later reaction consists of very long single crystalline Ga_2O_3 nanobelts and microscale single crystalline Ga_2O_3 sheets.
[24] R. S. Wagner, W. C. Ellis, Appl. Phys. Lett. 4, 89 (1964).
[25] T. J. Trentler et al., Science 270, 1791 (1995).
[26] G. W. Sears, Acta Metall. 3, 268 (1956).
[27] Bunshah, R., Ed., Handbook of Deposition Technologies for Films and Coatings (Park Ridge, New Jersey), 140-150, 198-202.
[28] Dai, Z. R., J. L. Gole, J. D. Stout, and Z. L. Wang, 2001, "Tin Oxide Nanowires, Nanoribbons, and Nanotubes," J. Phys. Chem. B, 1274-1279
[29] Dai, Z. R., Z. W. Pan, and Z. L. Wang, 2002, "Growth and structure evolution of novel tin oxide diskettes," J. Am. Chem. Soc., 8673-8680
[30] Dolbec, R., M. A. Khakani, A. M. Serventi, M. Trudeau, and R. G. Saint-Jacques, 2002, "Microstructure and physical properties of nanostructured tin oxide thin films grown by means of pulsed laser deposition," Thin Solid Films, 419, 230-236.
[31] Fouad, O. A., 2006, "Formation of Nanostructured Tin Oxide Semiconductors by a Simple Thermal Redox Process," Cryst. Res. Technol., 880-884
[32] J. LančokA., Santoni, M. Penza, S. Loreti, I. Menicucci, C. Minarini and M. Jelinek, 2005, "Tin oxide thin films prepared by laser-assisted metal–organic CVD: Structural and gas sensing properties," Elsevier B.V., 1057-1060
[33] Kim, J. S., M. Y. Huh, J. P. Ahn, 2007, "Effects of Particle Size on the Oxidation Behavior of Nanophase Tin Synthesized by Inert Gas Condensation," Trans Tech Publications, 9-12
[34] Li, Y., Y. Bando, and T. Sato, 2002, "Preparation of network-like MgO nanobelts on Si substrate," Chem. Phys. Lett. 359, 141-145.
[35] Peterson, G. P., 1994, "An Introduction to Heat Pipes," John Wiley and Sons Incorporated, 1-16

[36] Seung, Y. B., W. S. Hee, J. Park, H. Yang, and A. S. Se, 2002, "Synthesis and structure of gallium nitride nanobelts," Chem. Phys. Lett. 365, 525-529.

[37] Wang Z., and H. L. Li, 2002, "Highly ordered zinc oxide nanotubules synthesized within the anodic aluminum oxide template," Appl. Phys. A 74, 201-203.

[38] Wang, Z. L., and Z. W. Pan, 2002, "Nanobelts of semiconductive oxides: a structurally and morphologically controlled nanomaterials system," Int. J. Nanoscience 1, 41-45.

[39] Santos, G. N. C. "Synthesis of $Pb_xSn_{1-x}Te$ Semiconductor Crystals," De La Salle University, 1-34